IEEE Photonics Journal
An IEEE Photonics Society Publication

Open Access

Weak-Seed Induced Enhancement of Stimulated Raman Scattering in Distributed Side-Pumped Yb-Doped Fiber Amplifiers

Volume 12, Number 6, December 2020

Heng Chen
Jianqiu Cao
Aimin Liu
Zhihe Huang
Meng Wang
ZeFeng Wang
Xiaolin Wang
Jianbao Chen

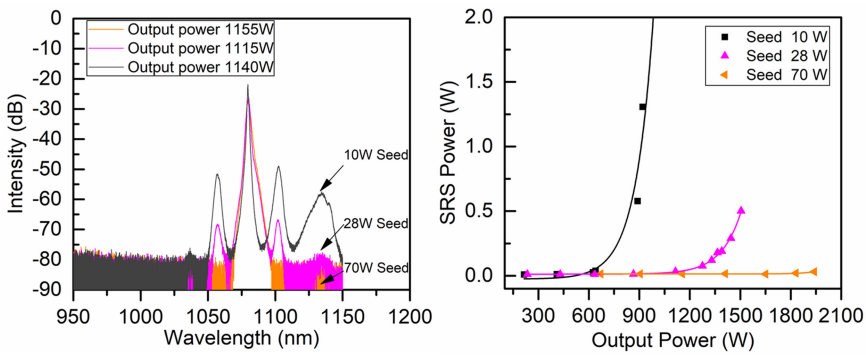

Weak-seed induced enhancement of stimulated Raman scattering

DOI: 10.1109/JPHOT.2020.3037501

Weak-Seed Induced Enhancement of Stimulated Raman Scattering in Distributed Side-Pumped Yb-Doped Fiber Amplifiers

Heng Chen,[1,2,3] **Jianqiu Cao**,[1,2,3] **Aimin Liu**,[1,2,3] **Zhihe Huang**,[1,2,3] **Meng Wang**,[1,2,3] **ZeFeng Wang**,[1,2,3] **Xiaolin Wang**,[1,2,3] **and Jianbao Chen**[1,2,3]

[1]College of Advanced Interdisciplinary Studies, National University of Defense Technology, Changsha 410073, China
[2]Hunan Provincial key Laboratory of High Energy Laser Technology, Changsha 410073, China
[3]Hunan Provincial Collaborative Innovation Center of High Power Fiber Laser, Changsha 410073, China

DOI:10.1109/JPHOT.2020.3037501

Manuscript received August 6, 2020; revised November 6, 2020; accepted November 9, 2020. Date of publication November 16, 2020; date of current version December 2, 2020. This work was supported by National Natural Science Foundation of China under Grant U20B2058. *(Heng Chen and Jianqiu Cao are co-first authors.)* Corresponding authors: Jianqiu Cao; Jinbao Chen (email: jq_cao@126.com; kdchenjinbao@aliyun.com).

Abstract: The effect of tens-of-Watt seed light on the stimulated Raman scattering (SRS) in a distributed side-pumped Yb-doped fiber amplifier is studied. By using two sorts of seed sources with the power smaller than 70 W, it is observed in experiment that the SRS can be enhanced by lowering the seed power. To the best of our knowledge, this is the first observation of the weak-seed enhancement of SRS in the distributed side-pumped Yb-doped fiber amplifier. In order to reveal the physical mechanism of the phenomenon, the numerical study is carried out. It is found that the Yb-gain at Raman wavelength, although much smaller than that at signal wavelength (i.e., 1080 nm), plays an important role in the phenomenon. It is also revealed that the weak-seed enhancement of SRS can only be presented when the dopant concentration is large enough (e.g., larger than 3×10^{25} in our numerical calculation). Besides, with more effective suppression of Raman seed, the weak-seed induced enhancement of SRS could be observed in a larger seed power range. The pertinent results and conclusion can provide significant guidance for designing high-power fiber lasers and amplifiers.

Index Terms: Fiber laser, fiber nonlinear optics, laser amplifiers.

1. Introduction

High-power Yb-doped fiber lasers and amplifiers have attracted much attention in the last two decades because of their outstanding characteristics such as compactness, robustness, good beam quality and high efficiency [1]–[6], and their wide applications in fields of industrial processing, medicine and scientific research. One topic driving their developments is how to up-scale their output powers. However, there are some physical obstacles limiting their power up-scaling [7]–[9], and stimulated Raman scattering (SRS) is just an important one of these obstacles.

In fact, the negative effect on kilo-Watt (kW) Yb-doped fiber lasers and amplifiers had been observed in [10]–[13]. It was found that the output efficiency will be dramatically lowered when the SRS was present. Then, SRS was considered as one important physical limitation to the power up-scaling of high-power Yb-doped fiber lasers, and pertinent studies became more and more heated [11], [14]–[24]. In order to make numerical studies, the SRS effect was introduced into the rate-equation model of Yb-doped fiber lasers and amplifiers [23]. Some (semi-) analytical formulas were also presented to predict the SRS threshold in high-power Yb-doped fiber amplifiers [18], [22]–[24].

With the development of pertinent studies, it was revealed that beside the Raman gain of Yb-doped fiber, the seed characteristics should also have non-negligible effects on the SRS in the high-power Yb-doped fiber amplifiers [12], [16], [25]. Some studies showed that the temporal instability of seed power can lower the SRS threshold of high-power fiber amplifiers [20]. Some methods to suppress the negative effect of seed instability were also presented, e.g., introducing the long passive fiber in the seed source [16] or optimize the bandwidth of seed source [20]. Another seed characteristic is the Raman noisy in the seed light. It was found that the Raman noisy can obviously enhance SRS in the high-power Yb-doped fiber amplifiers [18], which can be effectively lowered with the Raman filter such as the tilted fiber Bragg gratings (TFBGs) [15], [26] or long period gratings (LFBGs) [27]–[29]. Furthermore, the seed average power also plays an important role in SRS threshold. Both the theoretical and experimental studies revealed that the Raman light was proportional to the seed power [12], [20]. However, Ref. [30] also observed that the Raman light will decrease with the increment of seed power, but no explanation was given. Besides, no other reference was found to report the phenomenon similar to Ref. [30].

In recent years, the distributed side-pumped fiber amplifier becomes attractive. Actually, as early as 2004, the kilo-Watt (kW) distributed-pumped fiber amplifier (consisting of more-than-one bi-directional pumped sub-amplifiers) was studied numerically and its thermal advantage (low thermal load in active fiber) was revealed [24], [31]. It was also addressed that the SRS should be taken into account in the designation of kW distributed-pumped fiber amplifier [24]. Later, in 2019, the SRS threshold of distributed-pumped fiber amplifier was studied analytically and numerically [17], and it was also implied that the increment of seed power should lower the SRS threshold. In spite of that, the pertinent experimental study was not given yet.

In this paper, the effect of seed power on the high-power distributed side-pumped fiber amplifier will be experimentally studied. The distributed side-pumped fiber amplifier consists of two sub-amplifiers fabricated with the distributed side-coupled cladding-pumped (DSCCP) fiber [13], [32], [33]. Two sorts of seed sources are used in experiment. One is the single-mode fiber oscillator and the other is the oscillator with a long passive fiber for lowering the power instability. It is unexpected to find that, with both of two seeds, the SRS is weakened by increasing the seed power, which is different from all the reported theoretical or numerical predictions [14], [18], [20]. In order to deeply understand the experiment observation, the numerical study is carried out, with the help of which, the pertinent physical mechanism of the weak-seed enhancement of SRS is discussed.

2. Experimental Setup and Results

The experimental setup is given in Fig. 1. The distributed side-pumped fiber amplifier consists of two sub-amplifiers, where a 15-m long DSCCP ytterbium-doped fiber (YDF) is used in each sub-amplifier. Besides, the inset is the cross section of DSCCP fiber. The diameters of core 1 and inner-cladding 3 are both 250 μm, core 2 has a diameter of 25-μm diameter with a $\sim$0.065 numerical aperture (NA) and the diameter of outer cladding 4 is 650 μm. Pump light is provided by four wavelength-stabilized 976-nm laser diodes (LDs, the central wavelength is 976 $\pm$ 0.5 nm) through four pump ports (i.e., the core 1), then the pump light gradually couples into the inner-cladding 3 in form of the evanescent wave, and finally activating the Yb-ions in core 2. The smallest coiling diameter of the active fiber in the amplifier is 30 cm and no other mode control measures are taken.

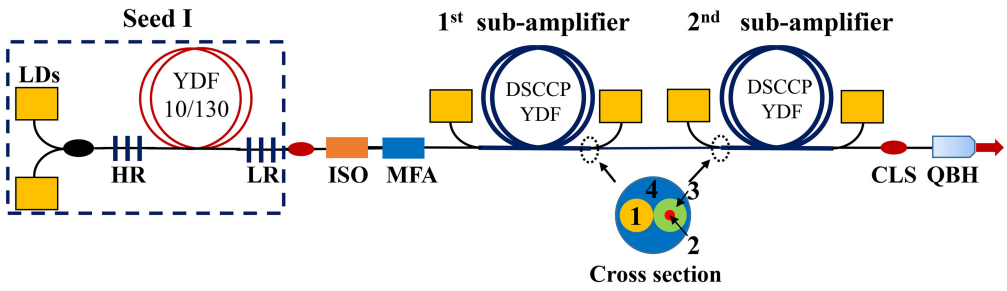

Fig. 1. The schematic of the all-fiber distributed side-pumped fiber laser (the inset is the cross section of DSCCP fiber). The quartz block header (QBH) with 9-m long passive fiber is spliced to the output ports to eliminate probable harmful feedbacks.

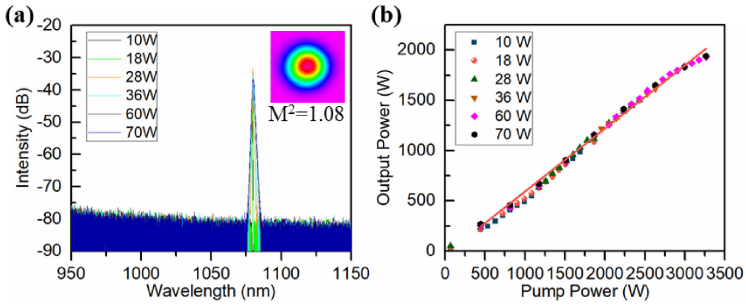

Fig. 2. (a) The spectra of seed I after the MFA, the inset is the beam profile at maximum power; (b) the laser output of amplifier at different seed power versus the pump power.

The configuration of seed source (seed I) is given in Fig. 1. A 13-m double cladding YDF with a core/inner-cladding diameter of 10/130 μm is used as the active fiber. Besides, the NA of active core is 0.07, which can guarantee the single mode operation. The pair of fiber Bragg gratings (FBGs) are centered at the wavelength of ~1080 nm (the 3-dB spectral bandwidths is 2 nm and 1 nm, respectively), and the reflectivity of HR FBG and OC FBG are 99% and 11%, respectively. After the seed source, a cladding light stripper (CLS) is utilized to strip out the residual pump light and an isolator (ISO) is incorporated to protect the seed laser source from the backward propagation light. Besides, a mode field adaptor (MFA) is employed to keep mode field diameter matched with DSCCP fiber. The output spectra of seed source after the MFA are shown in Fig. 2(a) and the inset is the beam profile at maximum power (e.g., 70 W, M^2~1.08). The pertinent 3-dB bandwidth increases from 0.16 nm to 1.29 nm with the seed power rises from 10 W to 70 W.

Then, the output characteristic of the amplifier is measured, where the seed power is set to 10 W, 18 W, 28 W, 36 W, 60 W and 70 W, respectively. The output powers of the amplifier corresponding to various seed powers are given in Fig. 2(b). It can be found that the output power increases linearly with the pump power and the slope efficiency is around 62% with various seed powers. Since the variation of seed power is limited (from 10 W to 70 W), the effect of seed power on output power is negligible.

The output spectra of the amplifier corresponding various seed power are given in Fig. 3, respectively. Once the signal output power exceeds the SRS threshold, the energy is transferred from signal wavelength (i.e., 1080 nm) to the Raman wavelength (i.e., 1134nm) with the increment of pump power. It can be seen that when the output power is around 640 W with the seed power of 10 W, the SRS light is observed (see Fig. 3(a)). Then, with the seed power increased to 18 W, the SRS light is first detected when the output power is about 850 when (see Fig. 3b). Further increasing the seed power from 28 W to 36 W, the SRS threshold raises significantly from 1115 W to 1615 W (see Fig. 3c–d). If the seed power up to 60 W and 70 W, the SRS light can be hardly observed even when the output power over 1900 W (see Fig. 3e-f). All these results imply that the threshold of SRS increases with the increment of seed power.

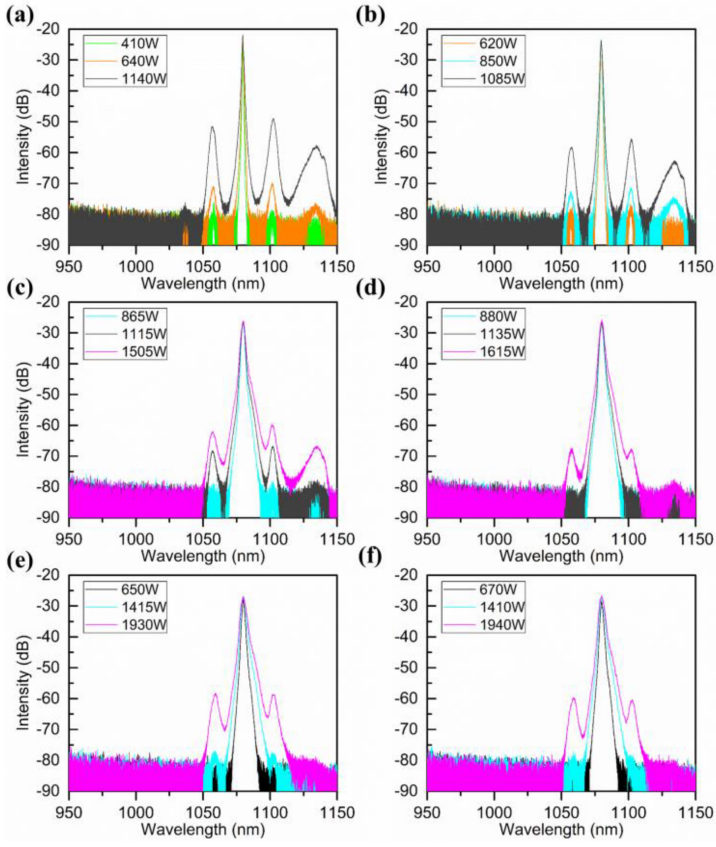

Fig. 3. The output spectra of amplifier with seed I, where the seed power is set to (a) 10 W, (b) 18 W, (c) 28 W, (d) 36 W, (e) 60 W, and (f) 70 W, respectively.

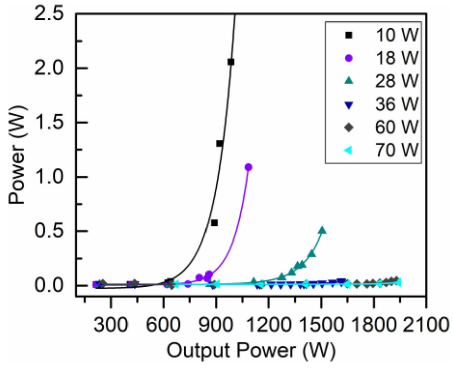

Fig. 4. The evolution of SRS power corresponding to various seed power.

In order to demonstrate the relationship between the SRS and seed power, the pertinent Raman power (estimated by integrating the output spectrum) corresponding various seed power are given in Fig. 4. It can be seen more clearly that more output power is needed to reach the SRS threshold with the increment of seed power. It can be also seen that when the output power beyond 640 W with the seed power of 10 W, the SRS power increased sharply and it can even reach the order of several watts at the output power of 900 W. when the seed power is increased to 18 W and 28 W, the SRS threshold is up to 850 W and 1115 W, respectively, and it is also on the order of watts at the output power of 1100 W and 1505 W. Then, further enhance the seed power, and

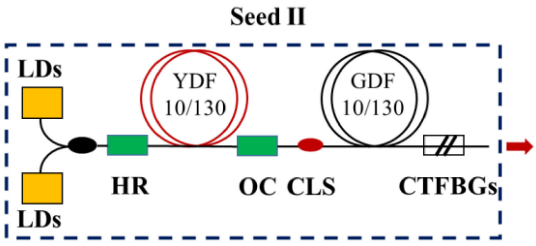

Fig. 5. The schematic of seed II. The Ge-doped fiber (GDF) is a common passive fiber with a core/inner-cladding diameter of 10/130 μm.

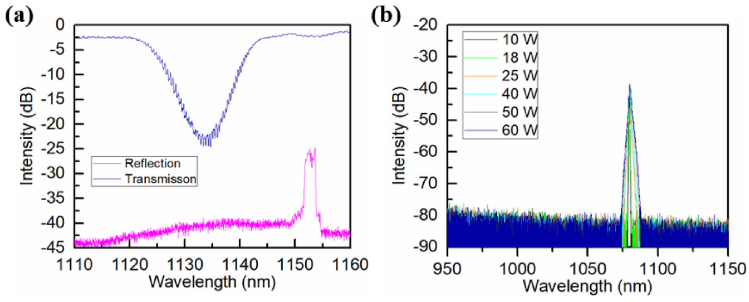

Fig. 6. (a) the reflection and transmission spectra of the TFBG; (b) The spectra of seed II after the MFA.

the thresholds will also increase. Thus, it can be concluded that the SRS should be enhanced by lowering the seed power.

Such a result is surprising because it is contradictory to all the theoretical and numerical predictions formerly reported. One possible reason is that the seed power instability become serious with lowering the seed power, which induces the enhancement of SRS [34]. In order to verify this reason, the seed source was improved (i.e., Seed II) as shown in Fig. 5. Firstly, we introduced a 115-m passive fiber which can suppress the seed power instability [16]. Then, a TFBG is also introduced to filter the Raman noisy, and its transmission and reflection spectra are shown in Fig. 6(a), the 3-dB bandwidth of transmission spectrum is 5.5 nm. Besides, the output spectra of the seed II are given in Fig. 6(b). The pertinent 3-dB bandwidth increases from 0.28 nm to 1.20 nm with the seed power rises from 10 W to 60 W, which is slightly wider than that of Seed I (see Fig. 2a) at the same power output.

The spectrum of amplifier with Seed II are measured, which is shown in Fig. 7. It can be seen that the SRS light is observed the output power of 690 W with the 10-W seed power injected (see Fig. 7a). Further increase the seed power to 18 W and 25 W, the SRS appears at the output power of 920 W and 1630 W, respectively (see Fig. 7b-c). While, the SRS light can be hardly observed even when the output power over 1900 W in Fig. 7d-f, since the seed power up to 50 W, 60 W and 70 W. However, by comparing these results in the case of Seed I (see Fig. 3a-d), it can be seen that all the thresholds with respect to the seed powers are higher than that of Seed I (with the threshold/seed power of 640 W/10 W, 850 W/18 W, 1115 W/ 28 W and 1615 W/36 W). Thus, the Seed II with a long passive fiber and a TFBG will help to increase the SRS threshold. However, similar to the result of seed I, it can be found that Raman light is still weakened by increasing the seed power.

Then, the variation of Raman power with output power are depicted in Fig. 8. It can be seen that the threshold of case with 10-W seed power injected is reached at the output power of 690 W, which is significantly lower than that of 18-W seed power injected. Then, with the higher seed power injected, the SRS threshold gets higher. Although the SRS growth is not obvious where the seed power are 50 W and 60 W, the result that the SRS should be enhanced by weakening the seed power is not varied. Moreover, by comparing with the results of Seed I (see Fig. 4), it can be

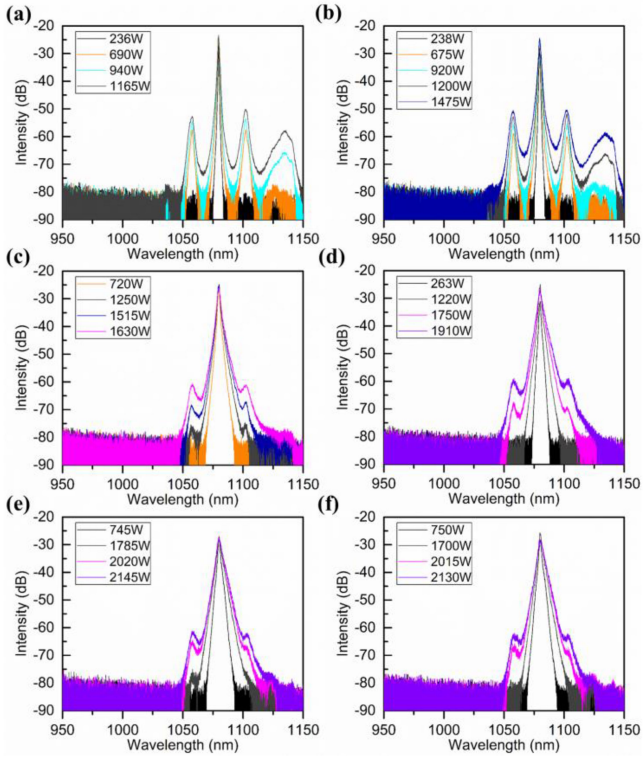

Fig. 7. The output spectra of amplifier with seed I, where the seed power are set to (a) 10 W, (b) 18 W, (c) 25 W, (d) 40 W, (e) 50 W, and (f) 60 W, respectively.

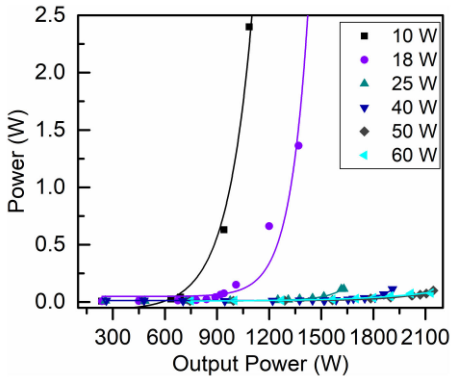

Fig. 8. The evolution of SRS power corresponding to various seed power.

seen clearly that the SRS is weakened and its threshold is elevated with Seed II at the same seed power. Considering that the power instability of Seed II is better than that of Seed I and both two seeds witness that the SRS is weakened by increasing the seed power, it can be inferred that the seed power instability should not be the key reason of this phenomenon.

3. Numerical Study

The anomalous effect of seed power on SRS drives us to think about whether there is other physical mechanism inducing the SRS enhancement by weak seed. Therefore, we carried out the numerical study. In order to remove the effect of seed power instability, the steady-state rate-equation model

is used, which is given as follows [35], [36].

$$\frac{N_2(z)}{N}=\frac{\Gamma_p\sigma_{ap}[P_p^+(z)+P_p^-(z)]\lambda_p+\Gamma_s\sigma_{as}P_s(z)\lambda_s++\Gamma_R\sigma_{aR}P_R(z)\lambda_R}{\Gamma_p(\sigma_{ap}+\sigma_{ep})[P_p^+(z)+P_p^-(z)]\lambda_p+\Gamma_s(\sigma_{as}+\sigma_{es})P_s(z)\lambda_s+\Gamma_R(\sigma_{aR}+\sigma_{eR})P_R(z)\lambda_R+hcA_c/\tau} \quad (1)$$

$$\pm\frac{dP_{pp}^{\pm}(z)}{dz}=-k_1P_{pp}^{\pm}(z)+k_2P_p^{\pm}(z)-\alpha_pP_p^{\pm}(z) \quad (2)$$

$$\pm\frac{dP_p^{\pm}(z)}{dz}=-\Gamma_p[\sigma_{ap}N-(\sigma_{ap}+\sigma_{ep})N_2(z)]P_p^{\pm}(z)-\alpha_pP_p^{\pm}(z)+k_1P_{pp}^{\pm}(z)-k_2P_p^{\pm}(z) \quad (3)$$

$$\frac{dP_s(z)}{dz}=-\Gamma_s[\sigma_{as}N-(\sigma_{as}+\sigma_{es})N_2(z)]P_s(z)-\alpha_sP_s(z)-\frac{\lambda_R}{\lambda_s}\frac{g_R}{A_{eff}}P_R(z)P_s(z)+2\Gamma_s\sigma_{es}N_2(z)\frac{hc^2}{\lambda_s^2}\Delta\lambda_s \quad (4)$$

$$\pm\frac{dP_R^{\pm}(z)}{dz}=-\Gamma_R[\sigma_{aR}N-(\sigma_{aR}+\sigma_{eR})N_2(z)]P_R^{\pm}(z)-\alpha_RP_R^{\pm}(z)+\frac{g_R}{A_{eff}}P_R^{\pm}(z)P_s(z)+2\Gamma_R\sigma_{eR}N_2(z)\frac{hc^2}{\lambda_R^2}\Delta\lambda_R. \quad (5)$$

Where the upper level population density and rare-earth ions dopant concentration are given by $N_2(z)$ and N, respectively. Γ_s,Γ_p and Γ_R are the filling factor of signal light, pump light and Raman light, respectively. λ_s, λ_p and λ_R are the wavelength of the signal light, pump light and Raman light, respectively. $\Delta\lambda_R$ and $\Delta\lambda_s$ represent the bandwidth of the Raman and signal light, respectively. $P_s(z)$, $P_{pp}^{\pm}(z)$, $P_p^{\pm}(z)$and $P_R^{\pm}(z)$ are the signal power, pump power in the pump core, pump power in the signal fiber and Raman power, respectively, where the plus and minus superscripts represent propagation along the positive or negative z directions, respectively. σ_{es},σ_{as}, σ_{ep}, σ_{ap},σ_{eR} and σ_{aR} are the emission and absorption cross sections of signal light, pump light and Raman light, respectively. α_s, $\alpha_p$and α_R characterize the loss of active fiber at the wavelengths of signal light, pump light and Raman light, respectively. k_1 is the averaged coupling coefficient of the pump light from the pump core to signal cladding, while k_2 is that from the signal cladding to the pump core [37]. A_c is the active core area, and A_{eff} is the effective mode area (roughly equal to the cross-section area of the core). τ is spontaneous lifetime. $g_R$characterizes the Raman gain coefficient. h is Planck's constant. $\boldsymbol{c}$ is the speed of light in vacuum. n is the refractive index of the active core.

Here, it should be noted that the Yb-gain at Raman wavelength and ASE are taken into account in the model. With the boundary conditions (Eq. 6) and parameter values given in Table 1, the model can be calculated and the pertinent results can be given.

$$\begin{aligned}P_s(0)&=P_{s0}\\P_R(0)&=P_{R0}\\P_{pp,i}^+(0)&=P_{p0,i}^+,\ i=1,2\\P_{pp,i}^-(L_i)&=P_{p0,i}^-,\ i=1,2.\end{aligned} \quad (6)$$

Where P_{s0} and P_{R0} are the values of the seeded signal power and seeded Raman power. $P_{p0,i}$represents the pumping power injected into the i^{th} sub-amplifier.

The numerical results are given in Figs. 9 and 10, it is interesting to find that the SRS can indeed be enhanced by lowering the seed power, although the enhancement is weaker than the experimental observation. However, such enhancement of SRS by lowering the seed power is not monotonous. From Fig. 9, it can be seen that the SRS enhancement can only be present when the seed power is weaker than some value (e.g., 150 W in Figs. 9a and 9b, 90 W in Fig. 9c and 70 W in Fig.9d). It means that with more effective suppression of Raman seed, the weak-seed induced enhancement of SRS could be observed in a larger seed power range. When the seed power is larger than the value, the SRS is not enhanced anymore, but weakened by lowering the seed power, which is coincident to formerly reported results given in [12], [14], [18], [20]. The same variation of SRS with seed power can also be revealed by Fig. 10 which shows that the largest SRS threshold can be obtained at some value of seed power. Here, SRS threshold is defined as the output power when a Raman output power that is 0.1% of the signal output power) [22].

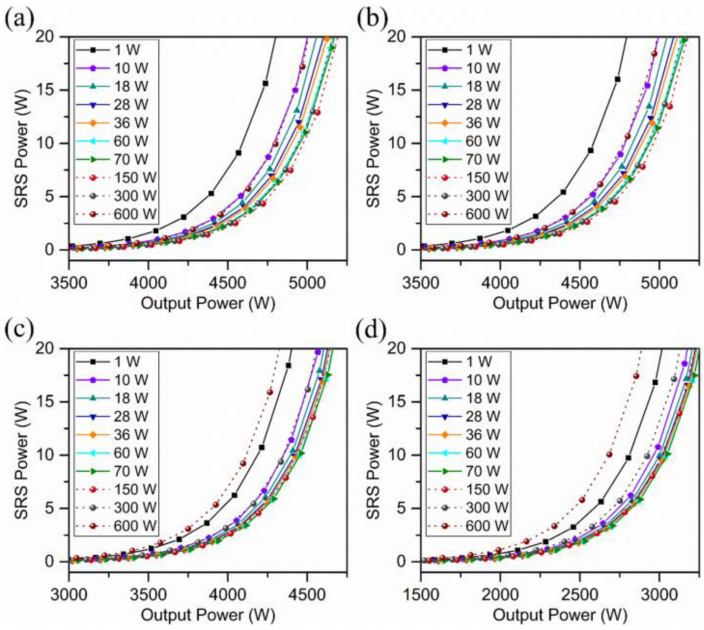

Fig. 9. The numerical results with seed power of 1 W,10 W,18 W,28 W,36 W,60 W,70 W,150 W, 300 W and 600 W, where the Raman seed is taken as (a) 0, (b) 10^{-8}, (c) 10^{-6}, and (d) 10^{-4}, respectively.

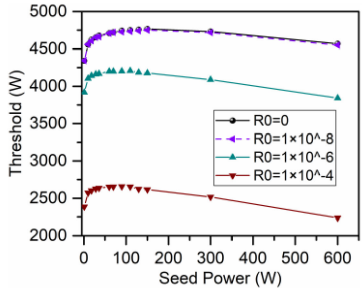

Fig. 10. The SRS threshold at various Raman seed (0, 10^{-8}, 10^{-6}, 10^{-4}) with respect to the seed power.

When the seed power is larger the value, the SRS threshold will not increase, but reduce with the increasing the seed power. Therefore, it means that the SRS enhancement induced by lowering the seed power can only present when the seed is weak enough. Therefore, it is named as the "weak-seed enhancement of SRS". From Fig. 10, it can be also found that the SRS threshold is almost the same with the 0 and 10^{-8}-W Raman seed. The reason is that the Raman seed is too weak and its effect on the SRS is negligible compared with the effect of spontaneous emission in the fiber amplifier [18]. Then, the SRS is mainly determined by the spontaneous emission and thus its threshold keeps almost unvaried with the seed power [18].

In order to reveal the physical mechanism inducing the results given in Fig. 10, we examine the effect of Yb-gain at Raman wavelength. Here, we neglect the Yb-gain related terms (i.e., the first term and last term in right side of Eq. (5)), and then, the Raman power should only be produced by SRS induced by the signal power (see the third term in right side of Eq. (5)). Then, the numerical calculation was made with the same parameter values given in Table 1 and the results are given in Fig.11. It can be known that without the Yb-gain at Raman wavelength, SRS will not be enhanced by weakening the seed power any more, and instead, it will be weakened monotonously by reducing the seed power. By comparing the results given in Fig. 10, it can be concluded that the Yb-gain at Raman wavelength plays an important role in the weak-seed enhancement of SRS, although it is much weaker than the Yb-gain at signal wavelength.

TABLE 1
Parameter Values Used in the Numerical Calculation

Parameters	Values	Parameters	Values	Parameters	Values
σ_{ap}	[38]	λ_s	1080 nm	α_s	1×10^{-3}
σ_{ep}	[38]	λ_p	976 nm	α_p	1×10^{-2}
σ_{as}	[38]	λ_R	1134 nm	α_R	1×10^{-3}
σ_{es}	[38]	$\Delta\lambda_s$	1 nm	n	1.45
σ_{aR}	[38]	$\Delta\lambda_R$	5 nm	Γ_s	0.85
σ_{eR}	[38]	τ	0.85 ms	Γ_p	0.01
A_{eff}	4.91×10^{-10} m^2	c	3×10^{8} m/s	N	1×10^{26}
g_R	1×10^{-13} m/W	h	6.626×10^{-34}		

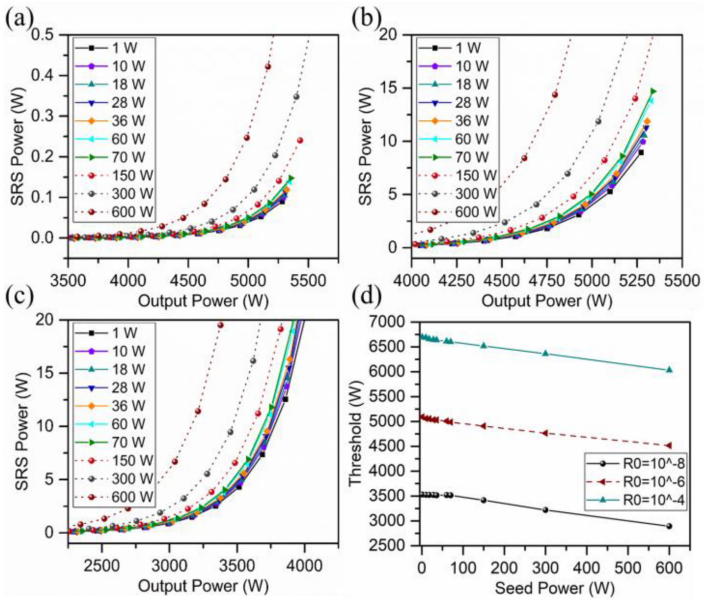

Fig. 11. The numerical results which ignore the Yb-gain at Raman wavelength ($N = 1 \times 10^{26}$), where the Raman seed is taken as (a) 10^{-8}, (b) 10^{-6}, and (c) 10^{-4}, respectively, and (d) shows the corresponding SRS thresholds via seed power.

Here, one thing should be noticed that the Yb-gain at Raman wavelength mentioned above is contributed by two parts. The first one is the gain induced by the population inversion of Yb-ion represented by the first term in the right side of Eq. (5). The second one is the gain contributed by the spontaneous emission (SE) related by the upper level population N2 of Yb-ion (i.e., the last term in the right side of Eq. (5)). Then, because the smaller seed power will induce higher upper level population N2 (see Eq. (1)), it will enhance both of two parts and thus enhance the Yb-gain at Raman wavelength. It is implied that although both of two parts are much smaller than the Yb-gain at signal wavelength, they should still be non-negligible when the seed power is weak. Actually, such an effect of small Yb-gain at Raman wavelength is not astonishing, because the enhancement of SRS caused by small Yb-gain was also considered in Refs. [39], [40].

Then, we examine the effect of dopant concentration (N) on the SRS enhancement, because it is crucial to the Yb-gain. The numerical results are given in Figs. 12 and 13. It can be seen that the weak-seed enhancement of SRS can only be present when the N is large than 3×10^{25}. When N is relatively small (e.g., 8×10^{24} and 1×10^{25} in Figs. 12a and 12b), the SRS will be weakened monotonously with the reduction of seed power, and the weak-seed enhancement of

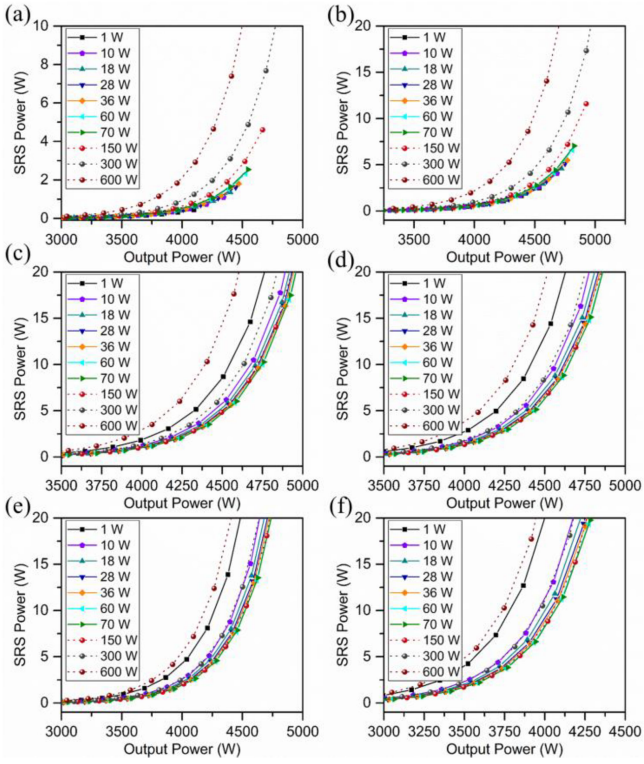

Fig. 12. The numerical results at various seed power, where the dopant concentration is taken as (a) 8 $\times$ 10^{24}, (b) 1 $\times$ 10^{25}, (c) 3 $\times$ 10^{25}, (d) 5 $\times$ 10^{25}, (e) 8 $\times$ 10^{25}, and (f) 2 $\times$ 10^{26}, respectively.

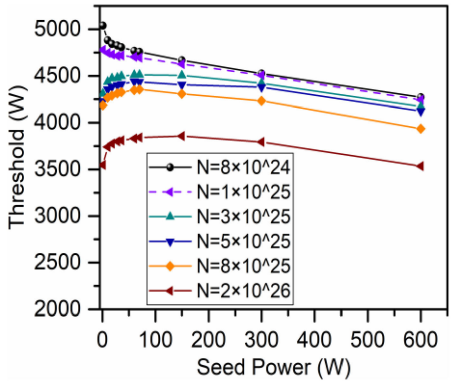

Fig. 13. The SRS threshold at various dopant concentration (8 $\times$ 10^{24}, 1 $\times$ 10^{25}, 3 $\times$ 10^{25}, 5 $\times$ 10^{25}, 8 $\times$ 10^{25}, 2 $\times$ 10^{26}) with respect to the seed power.

SRS cannot happen anymore. From Fig. 13, it can also be seen that the SRS threshold increases monotonously with lowering the seed power when N is relatively small. Thus, it can be concluded that the weak-seed enhancement of SRS can only appear when the dopant concentration is large enough.

At last, we would like make some discussions on the numerical results. The weak-seed enhancement of SRS can be observed both in experimental and numerical results. By comparing with the experimental results, it can be found that the numerical SRS threshold is generally larger than the experimental results. Besides, the numerical prediction of weak-seed enhancement of

SRS is generally weaker than the experimental observation. These differences may be induced by neglecting the seed power instability in the numerical model. Because the seed power instability will enhance SRS, such neglecting will make the numerical prediction of SRS threshold larger than the experimental results. Furthermore, because the instability of seed oscillator can also be enhanced with the reduction of seed power, the SRS with the lower seed power can be further enhanced which makes the weak-seed enhancement of SRS is more serious in experiment.

Another thing should be mentioned that besides the SRS, the IM-FWM can also be observed in the measured spectra given in Figs. 3 and 7. The pertinent study on IM-FWM is out of the scope of this paper, which will be carried out in the future.

4. Conclusion

The effect of seed power (no larger than 70 W) on the SRS of distributed side-pumped fiber amplifier is studied. By using two different seed sources, the weak-seed enhancement of SRS is observed in experiment. In order to reveal its physical mechanism, the numerical study is carried out. It is found that the weak-seed enhancement of SRS can indeed be present, and the Yb-gain at the Raman wavelength, although is weak, plays an important role in the phenomenon. It also revealed that the weak-seed enhancement of SRS can only happen when the dopant concentration is higher enough (e.g., higher than 3×10^{25} as the numerical result). However, It is unclear the impact of other parameters (e.g., Yb-fiber length, core size, nonlinear coefficient of Raman effects, etc.) on the "weak-seed enhancement of SRS", and further research is necessary. Then, the phenomenon can be understood as that when the seed power is too low to fully abstract the Yb-gain, the Raman noisy (including the Raman seed and Raman SE) can obtain sufficient Yb-gain to be amplified, and eventually the SRS will be enhanced. It means that the Yb-gain at Raman wavelength cannot be simply neglected even with the single wavelength as long as 1080 nm. Besides, the Yb-doped fiber with the dopant concentration higher than 3×10^{25} is generally used in practical high-power fiber amplifiers in order to shorten the cavity length for suppressing the nonlinear effect. Therefore, the seed power should not be too small and its optimization is indispensable in the designation of high-power fiber amplifiers. Moreover, it should be noted that the physical mechanism of weak-seed enhancement of SRS is not dependent on the type of active fiber, and the same phenomenon was witnessed in the double-cladding fiber laser with end-pumping technique [30].

Acknowledgment

The authors would like to thank 23th Research Institute of China Electronic Technology Group Corporation for useful help in fabricating the DSCCP fiber, and Z. Chen, K. Zhang and Q. Xiang for their useful help in experimental studies. They would also like to thank the anonymous reviewers for their valuable suggestions.

References

[1] J. Nilsson and D. N. Payne, "High-power fiber lasers," *Science*, vol. 332, no. 6032, pp. 921–922, 2011.
[2] C. Jauregui, J. Limpert, and A. Tünnermann, "High-power fibre lasers," *Nature Photon.*, vol. 7, no. 11, pp. 861–867, 2013.
[3] D. J. Richardson, J. Nilsson, and W. A. Clarkson, "High power fiber lasers: Current status and future perspectives," *J. Opt. Soc. Amer. B*, vol. 27, no. 11, pp. B63–B92, 2010.
[4] A. Tünnermann, "High-power cw fiber lasers present and future," *Laser Technik J.,* vol. 2, no. 2, pp. 54–56, 2005.
[5] A. Tünnermann, T. Schreiber, and J. Limpert, "Fiber lasers and amplifiers: An ultrafast performance evolution," *Appl. Opt.*, vol. 49, no. 25, pp. F71–F78, 2010.
[6] M. N. Zervas and C. A. Codemard, "High power fiber lasers: A review," *IEEE J. Sel. Topics Quantum Electron.*, vol. 20, no. 5, pp. 219–241, Sep. Oct. 2014.
[7] J. W. Dawson *et al.*, "Analysis of the scalability of diffraction-limited fiber lasers and amplifiers to high average power," *Opt. Express*, vol. 16, no. 17, pp. 13240–13266, 2008.
[8] J. Cao, S. Guo, X. Xu, J. Chen, and Q. Lu, "Investigation on power scalability of diffraction-limited Yb-doped fiber lasers," *IEEE J. Sel. Topics Quantum Electron.*, vol. 20, no. 5, pp. 373–383, 2014.

[9] H.-J. Otto, C. Jauregui, J. Limpert, and A. Tünnermann, "Average power limit of fiber-laser systems with nearly diffraction-limited beam quality," *SPIE LASE, Andreas*, 2016, vol. Proc. SPIE, Art. no. 97280E.
[10] L. B. Shaw *et al.*, "2.1 kW single mode continuous wave monolithic fiber laser," vol. 9344, 2015, Art. no. 93441G.
[11] T. Schreiber *et al.*, Analysis of stimulated raman scattering in cw kW fiber oscillators (SPIE LASE). *SPIE*, 2014.
[12] J. Wang, D. Yan, S. Xiong, B. Huang, and C. Li, "High power all-fiber amplifier with different seed power injection," *Opt. Express*, vol. 24, no. 13, pp. 14463–14469, Jun. 2016.
[13] H. Chen *et al.*, "Experimental investigations on multi-kilowatt all-fiber distributed side-pumped oscillators," *Laser Phys.*, vol. 29, no. 7, 2019, Art. no. 075103.
[14] J. Zhang *et al.*, "Optimization of seed power for suppression of stimulated raman scatting in all-fiber amplifiers," *Laser Phys. Lett.*, vol. 16, no. 3, 2019, Art. no. 035101.
[15] M. Wang, Z. Wang, L. Liu, Q. Hu, H. Xiao, and X. Xu, "Effective suppression of stimulated raman scattering in half 10 kW tandem pumping fiber lasers using chirped and tilted fiber bragg gratings," *Photon. Res.*, vol. 7, no. 2, pp. 167–171, 2019.
[16] T. Li, W. Ke, Y. Ma, Y. Sun, and Q. Gao, "Suppression of stimulated raman scattering in a high-power fiber amplifier by inserting long transmission fibers in a seed laser," *J. Opt. Soc. America B*, vol. 36, no. 6, pp. 1457–1465, 2019.
[17] H. Du, J. Cao, H. Chen, Z. Huang, and J. Chen, "Analytical study on the stimulated raman scattering threshold in distributed-pumped fiber amplifiers," *Appl. Opt.*, vol. 58, no. 8, pp. 2010–2020, 2019.
[18] H. Ying, J. Cao, Y. Yu, M. Wang, Z. Wang, and J. Chen, "Raman-noise enhanced stimulated raman scattering in high-power continuous-wave fiber amplifier," *Optik - Int. J. Light Electron Opt.,* vol. 144, pp. 163–171, 2017.
[19] G. Brochu, A. Villeneuve, M. Faucher, M. Morin, F. Trépanier, and R. Dionne, SRS modeling in high power CW fiber lasers for component optimization (SPIE LASE). SPIE, 2017.
[20] W. Liu, P. Ma, H. Lv, J. Xu, P. Zhou, and Z. Jiang, "General analysis of SRS-limited high-power fiber lasers and design strategy," *Opt. Express*, vol. 24, no. 23, pp. 26715–26721, 2016.
[21] T. Zhu, X. Bao, L. Chen, H. Liang, and Y. Dong, "Experimental study on stimulated rayleigh scattering in optical fibers," *Opt. Express*, vol. 18, no. 22, pp. 22958–22963, 2010.
[22] C. Jauregui, J. Limpert, and A. Tünnermann, "Derivation of raman threshold formulas for CW double-clad fiber amplifiers," *Opt. Exp.*, vol. 17, no. 10, pp. 8476–8490, 2009.
[23] Y. Wang, "Stimulated raman scattering in high-power double-clad fiber lasers and power amplifiers," *Opt. Eng.*, vol. 44, no. 11, pp. 1–12, Dec. 2005.
[24] Y. Wang, C.-Q. Xu, and H. Po, "Analysis of raman and thermal effects in kilowatt fiber lasers," *Opt. Commun.*, vol. 242, nos. 4-6, pp. 487–502, 2004.
[25] H. Xu, M. Jiang, C. Shi, P. Zhou, G. Zhao, and X. Gu, "Spectral shaping for suppressing stimulated-Raman-scattering in a fiber laser," *Appl. Opt.*, vol. 56, no. 12, pp. 3538–3542, 2017.
[26] M. Wang, Z. Li, L. Liu, Z. Wang, and X. Xu, "Suppression of stimulated raman scattering in two-stage high-power 1090 nm fibre amplifier using chirped and tilted fibre bragg gratings," *Laser Phys.*, vol. 28, no. 12, 2018, Art. no. 125102.
[27] K. Jiao, H. Shen, Z. Guan, F. Yang, and R. Zhu, "Suppressing stimulated raman scattering in kW-level continuous-wave MOPA fiber laser based on long-period fiber gratings," *Opt. Express*, vol. 28, no. 5, pp. 6048–6063, 2020.
[28] D. Nodop, C. Jauregui, F. Jansen, J. Limpert, and A. Tünnermann, "Suppression of stimulated raman scattering employing long period gratings in double-clad fiber amplifiers," *Opt. Lett.*, vol. 35, no. 17, pp. 2982–2984, 2010.
[29] F. Jansen, D. Nodop, C. Jauregui, J. Limpert, and A. Tünnermann, "Modeling the inhibition of stimulated raman scattering in passive and active fibers by lumped spectral filters in high power fiber laser systems," *Opt. Express*, vol. 17, no. 18, pp. 16255–16265, 2009.
[30] C. Shi *et al.*, "Experimental study of output characteristics of Bi-directional pumping high power fiber amplifier in different pumping schemes," *IEEE Photon. J.*, vol. 9, no. 3, pp. 1–10, Jun. 2017.
[31] Y. Wang, C.-Q. Xu, and H. Po, "Thermal effects in kilowatt fiber lasers," *IEEE Photon. Technol. Lett.*, vol. 16, no. 1, pp. 63–65, Jan. 2004.
[32] H. Chen *et al.*, "Experimental investigations on TMI and IM-FWM in distributed side-pumped fiber amplifier," *IEEE Photon. J.*, vol. 12, no. 3, pp. 1–13, Jun. 2020.
[33] Z. Huang *et al.*, "A kilowatt all-fiber cascaded amplifier," *IEEE Photon. Technol. Lett.*, vol. 27, no. 16, pp. 1683–1686, Aug. 2015.
[34] W. Wang, J. Leng, Y. Gao, S. Guo, and Z. Jiang, "Influence of temporal characteristics on the power scalability of the fiber amplifier," *Laser Phys.*, vol. 25, no. 3, 2015, Art. no. 035101.
[35] Z. Huang, J. Cao, S. Guo, J. Chen, and X. Xu, "Comparison of fiber lasers based on distributed side-coupled cladding-pumped fibers and double-cladding fibers," *Appl. Opt.*, vol. 53, no. 10, pp. 2187–2195, 2014.
[36] Z. Huang, J. Cao, S. Guo, J. Chen, X. Xu, and J. Leng, "Model of distributed side-coupled cladding-pumped fiber lasers," *Adv. Solid-State Lasers Congr.*, p. ATu3A.27, 2013.
[37] Z. Huang, J. Cao, S. Guo, J. Hou, and J. Chen, "The characteristics of pump light in side-coupled cladding-pumped fibers," *Opt. Fiber Technol.*, vol. 19, no. 4, pp. 293–297, 2013.
[38] R. Paschotta, J. Nilsson, A. C. Tropper, and D. C. Hanna, "Ytterbium-doped fiber amplifiers," *IEEE J. Quantum Electron.*, vol. 33, no. 7, pp. 1049–1056, Jul. 1997.
[39] Q. Xiao *et al.*, "Bidirectional pumped high power raman fiber laser," *Opt. Express*, vol. 24, no. 6, pp. 6758–6768, Mar. 2016.
[40] H. Zhang, H. Xiao, P. Zhou, X. Wang, and X. Xu, "High power Yb-Raman combined nonlinear fiber amplifier," *Opt. Express*, vol. 22, no. 9, pp. 10248–10255, 2014.